COLLIDING STELLAR WINDS: X-RAY EMISSION AND INSTABILITIES

IAN R. STEVENS
School of Physics and Space Research, The University of Birmingham, Edgbaston, Birmingham B15 2TT, U.K.

Abstract. Colliding stellar winds are an important part of early-type binaries. In this paper I discuss the phenomenon, concentrating mainly on the basic hydrodynamics of colliding winds, and the physics of X-ray emission. The following topics are covered:
1) Basic physics: The basic characteristics of the shock-produced thermal X-ray emission, and discuss general trends of X-ray emission from colliding wind binaries (CWBs).
2) Hydrodynamic simulations: Recent calculations have found that the interface in colliding winds is usually dynamically unstable, with three distinct instabilities.
3) Gamma Velorum: recent *ROSAT* observations give much insight into colliding winds. I discuss recent hydrodynamic calculations pertaining to these observations.
4) Radiation Hydrodynamics in CWBs: Recent calculations have included the effects of both radiation fields on the wind hydrodynamics in colliding wind systems.

Key words: stars: Wolf-Rayet – X-rays – colliding winds

1. Introduction

Although the concept of colliding stellar winds in early-type binaries has been around for quite a while (*e.g.*, Prilutskii & Usov 1976), only recently has considerable progress been made been made in identifying observational signatures of colliding winds and in our theoretical understanding of the phenomenon. However, many significant open questions remain, and our knowledge of the hydrodynamics of such systems remains sketchy.

In this paper, in addition to reviewing the basic physics of colliding wind, I shall discuss some recent results on the hydrodynamics of colliding stellar winds in WR+O-star systems. This will have a mainly theoretical slant, but I shall also discuss the relevance of theoretical calculations to interpreting observational data on CWBs.

2. Basic physics

In WR+O-star systems, both stars have massive, supersonic winds. These wind collide, forming a double shock structure with a region of hot gas sandwiched between the shocks, subdivided by a contact discontinuity (Fig. 1). For material passing through a strong shock, the post-shock gas temperature is $kT_s = \frac{3}{16}\bar{m}v^2$ with $\bar{m}$ the mean particle mass ($\sim 10^{-24}$ g for solar abundances). This expression can be restated as $kT_s(\text{ keV}) \sim 1.2\ v_8^2$ with v_8 being the wind velocity at the shock in units of $10^8\,\text{cm s}^{-1}$.

K. A. van der Hucht and P. M. Williams (eds.), Wolf-Rayet Stars: Binaries, Colliding Winds, Evolution, 486–494.

In WR+O systems this means that the characteristic post-shock temperature is of order a few keV. As a consequence. the shocked gas caused by the wind collision will emit mainly at X-ray energies. Thus, while colliding winds will have signatures at different energies (γ-rays, Eichler & Usov 1993; UV, St-Louis *et al.* 1993) colliding winds will be directly visible by their thermal X-ray emission. To date, identifying unambiguous signatures of colliding winds has posed problems, particularly because of the confusion between colliding wind X-ray emission and intrinsic emission from shocks within the wind.

Wind momentum ratio $\mathcal{R}$

There are two parameters that can give a basic description of colliding wind. The momentum ratio $\mathcal{R}$* of the winds in a CWB is defined as:

$$\mathcal{R} = \left[\frac{\dot{M}\,(WR)v_\infty(WR)}{\dot{M}\,(O)v_\infty(O)}\right]^{1/2} \tag{1}$$

In WR+O-star systems the WR wind tends to have more momentum ($\mathcal{R} \sim 3-6$), and the O-star wind is contained within a cone of opening half-angle θ. Eichler & Usov (1993) give a useful analytic formula for θ

$$\theta\ (\text{degrees}) \sim 120\left(1 - \frac{\mathcal{R}^{-2/5}}{4}\right)\mathcal{R}^{-2/3}. \tag{2}$$

Cooling parameter χ

Another important factor in determining the structure of colliding winds is the degree to which the post-shock wind can cool. If the post-shock flow-time is much greater than a dynamical timescale then the post-shock flow is unable to cool substantially (*i.e.,* is essentially adiabatic) the post-shock region will consist of a pressure supported region of hot diffuse gas. On the other hand, if the cooling timescale is short compared to a dynamical timescale then the post-shock regions collapses into a dense shell of material, primarily constrained by ram pressure. We define a cooling parameter χ as

$$\chi = \frac{t_{cool}}{t_{dyn}} \approx \frac{v_8^4 d_{12}}{\dot{M}_{-7}} \tag{3}$$

where d_{12} is the distance to the contact discontinuity in units of 10^{12} cm, and $\dot{M}_{-7}$ is the mass loss rate in units of 10^{-7} $M_\odot yr^{-1}$. For dense post-shock material (*i.e.,* close binaries) the wind material will cool, while for wide binaries the post-shock material will be adiabatic. In § 3 we discuss

* Note, that the parameter η is also used by some authors, with $\eta = \mathcal{R}^{-2}$

https://doi.org/10.1017/S0074180900202519 Published online by Cambridge University Press

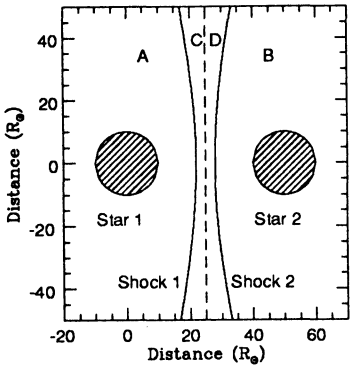

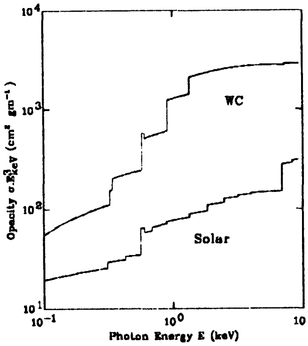

Fig. 1. Sketch of a CWB of identical stars with isotropic winds. The unshocked parts of the winds of stars 1 and 2, labelled A and B respectively, are bounded by two opposing shock fronts represented by the solid lines. In the hot region in between, regions C and D of shocked material from stars 1 and 2, respectively, are separated by a contact discontinuity represented by the dashed line.

Fig. 2. The effect of composition on the opacity of the wind material. The two cases shown are for solar type abundances and for values appropriate for the WC phase of WR evolution.

how the structure of the intershock region depends on the cooling parameter χ.

It is possible to obtain simple estimates of the X-ray luminosity from colliding winds. In the adiabatic case $\chi \gg 1$

$$L_x \propto \dot{M}^2 v^{-3.2} D^{-1} (1+\mathcal{R})/\mathcal{R}^4 \tag{4}$$

and in the isothermal limit $\chi \ll 1$ $L_x = f\dot{M}\,v^2$; all the shocked wind KE is thermalized and radiated. The function f is approximately given by $f \sim \mathcal{R}^{-2}$. For large values of $\mathcal{R}$ only a small portion of the dominant wind passes through the shock surface, while a very large portion of the lesser wind does, and the lesser wind may dominate the X-ray emission.

These two estimates are for the total X-ray luminosity. In reality, absorption by the stellar wind greatly affects the observed spectrum. A characteristic value for the absorbing column in CWBs is given by

$$\bar{N}_H \left(\mathrm{cm}^{-2}\right) \sim 5 \times 10^{21} \left(\frac{\dot{M}_{-7}}{v_8}\right) \left(\frac{1+\mathcal{R}}{\mathcal{R}}\right) d_{12}^{-1} \,. \tag{5}$$

In order to calculate the expected X-ray spectra of a CWB including absorption it is necessary to calculate detailed hydrodynamic models. In addition, these simulations have revealed a wealth of interesting dynamical phenomena (Stevens *et al.* 1992, hereafter SBP).

3. Hydrodynamic simulations

In SBP we reported on a set of 2-D hydrodynamic calculations of CWBs. These calculations demonstrated how complex a phenomenon colliding stellar winds are. Some important considerations from these calculations are given in this section.

3.1 Composition effects

One significant complication in models of WR+O-star binary systems is the composition of the wind material. This affects the model in two main ways:

1. X-ray emission: Different abundances have different emission characteristics (and hence different cooling curves). For example, abundances appropriate for WC stars have very enhanced C and O, which in turn gives rise to enhanced line emission (see SBP). Other things being equal WR abundance material radiates more of its thermal energy.
2. Different abundances also affect the absorption coefficient. WR wind material has enhanced CNO abundances. Because the CNO elements are efficient absorbers in the energy range $0.5 - 4$ keV this results in very enhanced absorption over solar abundances in the *ROSAT* waveband (also WC material is a more efficient absorber than WN material). A comparison of the absorption coefficients for solar and WC material is shown in Fig. 2). At 1 keV the absorption coefficient for WC material is ~ 20 that for solar abundance material. This has a profound impact on the visibility of X-rays from WC stars (see § 4).

3.2 Instabilities

In the simulations of SBP, three instabilities were discovered, the Kelvin-Helmholtz instability, a 'thin-shell' instability and a 'ram pressure' instability. All three are likely to play a role in CWBs.

3.2.1 Kelvin Helmholtz instability

This is the easiest to understand, many examples of which being commonly found in nature or generated in the laboratory (*i.e.*, wind generated water waves). If there is a velocity shear along the contact surface between two fluids then any perturbation will tend to grow. The growth time for the KH instability is

$$t_{KH} \approx \frac{\lambda}{u_1 - u_2} \left(\frac{\rho_1 + \rho_2}{2\pi\sqrt{\rho_1 \rho_2}} \right) , \tag{6}$$

where λ is the wavelength of the perturbation, ρ_1, ρ_2 are the densities on the two sides of the contact discontinuity, and $u_2 - u_1$ is the difference of tangential flow velocities along the two sides of the contact discontinuity. This timescale will be replaced by the wind flow timescale, D/v, when the

https://doi.org/10.1017/S0074180900202519 Published online by Cambridge University Press

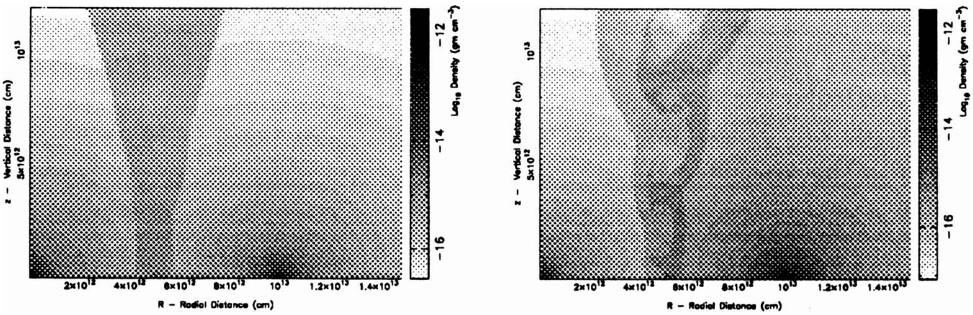

Fig. 3. The Kelvin-Helmholtz instability in colliding wind systems. Shown are two simulations both with a momentum ratio $\mathcal{R} = 1$ but with different wind velocities. In the left simulation $v_1 = 1.1v_2$ while in the right $v_1 = 2v_2$. Note the stronger growth of the instability in the right panel.

instability grows nonlinear and saturates. This instability will be found in very wide binary systems such as HD 193793 (WR140). Because wind terminal velocities of WR and O-type stars are broadly similar the velocity shear will tend to be quite small. In HD 193793 the ratio of terminal velocities is ~ 1.1, and growth times will be long. However, KH instabilities should be present though unlikely to have observable signatures.

3.2.2 Thin-shell instabilities

In addition to the KH instability, two distinct thin-shell instabilities where found when one or both sides of the postshock flow was able to radiate sufficiently to form a dense, cool shell.

Vishniac type instability

This instability occurs when one wind is adiabatic and the other is isothermal. This instability is related (but not identical) to the blast wave instability discussed by Vishniac (1983). This situation will occur in some WR+O binaries (§ 4), as well as in symbiotic systems.

Ram pressure instability

This instability, dubbed the 'ram pressure instability', will occur in close binary systems, such as V444 Cyg, where the post-shock wind density is large enough to allow radiative cooling to occur swiftly.

This instability has been carefully studied, both analytically and numerically by Dgani *et al.* (1993) and Dgani & Soker (1994), who found that this situation is indeed unstable to both tangential and radial perturbations. This instability may well have impart an intrinsic variability to the X-ray emission on a dynamical timescale. However, it is likely that this will be small and masked by orbital orientation effects.

https://doi.org/10.1017/S0074180900202519 Published online by Cambridge University Press

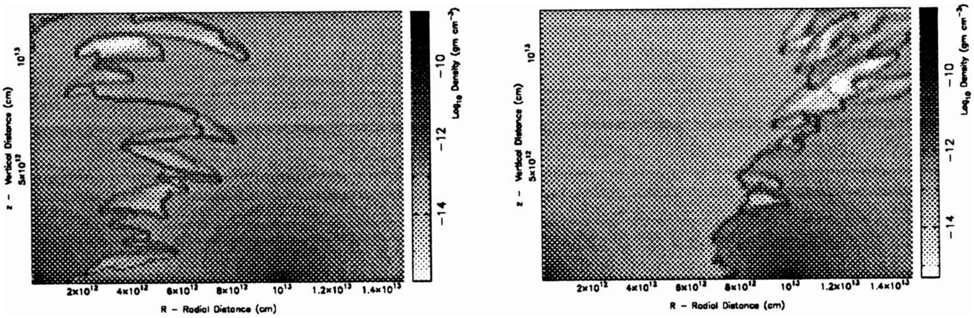

Fig. 4. **Ram pressure instability: Two simulations are shown, one with identical winds (left panel), the other with $\mathcal{R} = 3.2$ (right panel)**

4. Gamma Velorum

Recent *ROSAT* observations of γ Vel (WC8+O9I, orbital period 78.5 days), discussed by Willis *et al.* (these proceedings), have found some extreme variability that provides us with the best opportunity to date for studying colliding winds at X-rays energies. To summarise; γ Vel was observed 13 times with *ROSAT*. For most of the orbit a soft, low luminosity source was observed. However, when the O-star is in front of the WR star ($\phi = 0.4-0.6$) the X-ray flux increases by $\gtrsim 4\times$ ($L_x \sim 10^{32}$ ergs s^{-1}), with an additional hard ($kT \geq 2$ keV) component.

We believe that the hard component is colliding wind emission, and that in γ Vel we have an unprecedented view of colliding wind activity in such a close binary system. To back up this claim we have calculated several 2-D hydro models of γ Vel, and used them to calculate X-ray lightcurves.

The 'Standard model' was calculated with parameters from St-Louis *et al.* (1993) ($\dot{M}(WR) = 8.8 \times 10^{-5}$ M$_\odot$yr^{-1}, $\dot{M}(O) = 1.3 \times 10^{-6}$ M$_\odot$yr^{-1}, $v_\infty(WR) = 1520$ km s^{-1} and $v_\infty(O) = 2370$ km s^{-1}). Of note is the large WR mass-loss rate, and the binary eccentricity ($e = 0.4$); the separation varying from 180 R$_\odot$ to 420 R$_\odot$.

In Fig. 5 we show the 'Standard Model' simulation at periastron. Because of its large $\dot{M}$ the WR wind is strongly cooled, while the O-star wind is partially cooled. We have calculated the X-ray lightcurve for this model in the *ROSAT* waveband (0.1 – 2.5 keV, see Fig. 6). The following points should be noted:

- The total intrinsic X-ray luminosity (ignoring attenuation) is large $\sim 10^{36}$ ergs s^{-1}, though much smaller than the total wind KE. However, the majority of this flux is absorbed by the wind.
- The WR wind is an *extremely* efficient absorber of X-rays, both because of its composition and density. At phases when the line-of-sight passes through the WR wind the low energy cut-off is at several keV

https://doi.org/10.1017/S0074180900202519 Published online by Cambridge University Press

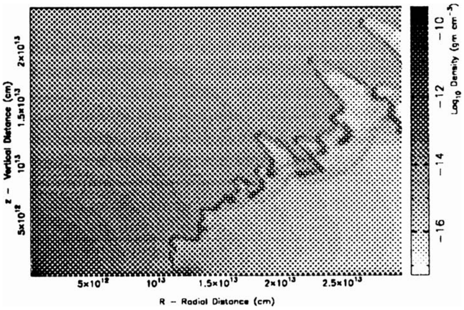

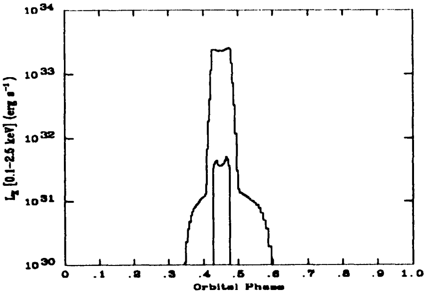

Fig. 5. 2-D hydrodynamic simulation of γ Vel at periastron. This is the 'Standard Model'. Note the post-shock gas is strongly cooled, particularly for the WR wind.

Fig. 6. X-ray lightcurves for two γ Vel simulations. The higher curve is for the 'Standard Model', which overestimates the observed X-ray flux by an order of magnitude. The lower curve is for a model with a reduced O-star wind velocity.

and virtually no X-rays from the colliding winds escape in the *ROSAT* waveband. What X-ray emission is seen is probably caused by the same process that causes X-ray emission in single early-type stars.

- At phases when the O-star is in front the low energy cut-off drops down into the *ROSAT* waveband, and colliding wind X-ray emission is seen, as a hard highly absorbed component superimposed on the soft component.
- The opening half-angle of the O-star star wind from the simulations is $\theta \sim 20° - 30°$ in rough agreement with the portion of the orbit when the X-ray flux is enhanced.
- The 'standard model' substantially overestimates the luminosity around periastron by an order of magnitude or so (see Fig 6).
- Better agreement can be obtained by lowering the O-star wind velocity to $\sim 1500\,\mathrm{km\ s^{-1}}$. This increases the O-star wind density and the absorbing column, reducing the amount of X-ray emission seen at phases $\sim 0.4 - 0.6$ to $\sim 10^{32}\,\mathrm{ergs\ s^{-1}}$.

There are good physical grounds for expecting a model with a lower O-star velocity to be are more accurate representation. Firstly, the WR wind dominates the system ($\mathcal{R} = 6.5$ for γ Vel). At periastron, when the binary separation is only $\sim$ 180 $R_\odot$, the shock surface will lie very close to the photosphere of the O-star, and as a consequence the O-star wind will not have sufficient room to reach terminal velocity. In addition, when account is made of the radiation hydrodynamics of the system, including the effect of both stars radiation fields, then the O-star wind velocity will be further suppressed (see § 5). To investigate this further will require improved hydrodynamic models incorporating the effects of radiative acceleration.

https://doi.org/10.1017/S0074180900202519 Published online by Cambridge University Press

5. Radiation hydrodynamics in CWBs

While the hydro simulations described in the § 3 and 4 are complex, the actual wind dynamics in CWBs will be even more complex, with two winds both being driven by the radiation pressure of both stars. In very wide systems ignoring this effect is probably valid. For example, in HD 193793 both winds have reached terminal velocity long before the radiation field of the companion star will be able to influence its dynamics.

The situation becomes a good deal more complicated in closer binary systems, such as V444 Cyg (WN5 +O6; orbital period $\sim$ 4.2 days). Here both radiation fields will contribute to the wind dynamics. The inclusion of this mechanism may provide an answer to the question of why theoretical model overestimate the X-ray temperature and luminosity of close CWBs. In the example of V444 Cyg, the WR wind terminal velocity is $\sim 1500\,\mathrm{km\ s^{-1}}$. This corresponds to an postshock X-ray temperature of $\sim$ 3 keV, compared to the observed 1 keV.

In Stevens & Pollock (1994) we have reported on new radiation hydrodynamic calculations of the dynamics of stellar winds under the influence of two radiation fields. These calculations are based on the Castor *et al.* (1975) formalism for stellar winds. Using V444 Cyg as an example we have calculated the dynamics of the winds on the binary line-of-centers. We find that when the effect of radiation pressure from the O-star is included the WR wind velocity at the point where the winds collide (on the binary line-of-centers) is $\sim$ 2 times lower than expected from single star models. This in turn means that the post-shock X-ray temperature when this effect is included is $\sim$ 1 keV, in line with X-ray observations. In contrast, if the binary system is very wide (as in the case of HD 193793) the radiation pressure on the O-star will have basically no effect on the dynamics, and both winds will be essentially at their terminal velocities when they collide.

In order to develop these ideas further it will be necessary to incorporate them into detailed 2-D hydro codes. However, once completed, this will give us a much more powerful tool to investigate colliding winds in close binary systems.

References

Castor, J.I., Abbott, D.C., Klein, R.I. 1975, *ApJ* **195**, 157
Dgani, R., Walder, R., Nussbaumer, H. 1993, *A&A* **267**, 155
Dgani, R., Soker, N. 1994, *A&A* **282**, 54
Eichler, D., Usov, V. 1993, *ApJ* **402**, 271
Prilutskii, O., Usov, V. 1976, *Sov. Astron.* **20**, 2
St-Louis, N., Willis, A.J., Stevens, I.R. 1993, *ApJ* **415**, 298
Stevens, I.R., Blondin, J.M., Pollock, A.M.T. 1992, *ApJ* **386**, 265 (SBP)
Stevens, I.R., Pollock, A.M.T. 1994, *MNRAS* in press
Vishniac, E. T. 1983, *ApJ* **274**, 152

DISCUSSION:

Marchenko: Maybe, we have one additional proof in a favor of the instabilities arising in the bow shock zone. In my talk yesterday I have shown that there are two components of the bow shock which affect the line profile: one is in emission, the other one is in absorption. And, the absorptions tend to be much more variable. We can explain this quite naturally, assuming that the emission is produced nearby the discontinuity surface due to fast recombination. Due to cooling (much slower than recombination) the bow shock absorption is formed further out, where the instabilities play the major role.

Stevens: I think these observations are particularly exciting and have great potential for helping us to understand the dynamics of colliding winds.

Nussbaumer: How is the spatial distribution of emission and absorption of the soft X-rays in your model of γ Vel? Is it mostly confined to the center of the system, or how far out are the essential processes happen?

Stevens: The hardest X-ray emission comes from a relatively small region on the line of centers of the system. Softer emission comes from further out. Absorption comes from a large spatial region. Unfortunately, I do not have useful numbers to hand.

Owocki: Two comments: 1. You mentioned the need to include the effect of line-driving in the wind flows. Of course, this is best first done with the local CAK form: that leads to smooth, stable acceleration. Eventually, though, I think one needs to consider the non-local line-force form that gives rise to the line-driven instability, with its associated reverse shocks, clumps, etc. As discussed in general terms by Sebastian Lepine's talk, and described by Cherepashchuk and others, this clumping may have significant effects on the wind collision structure.

2. Regarding rotation, one of the most interesting recent ideas is the Wind Compressed Disks from rotating stars. I should think that in close binary systems, the accelerating wind may also be deflected into a disk, with again important consequences for the wind collision.

Gies: In close binary systems, at what wavelengths might we see eclipse effects due to the occultations by the stellar disks?

Stevens: Potentially at the highest X-ray energies. The highest X-ray temperatures will occur on the binary line of centers where potentially they will be occulted in an eclipsing system. In reality X-ray emission from colliding wind systems will be very complicated and this effect may well not be observable.

Usov: If the stellar winds are the same, it is natural to expect that the gas velocity is the same on both sides of the contact surface. In this case, what is the reason for plasma instabilities near the contact surface?

Stevens: The "ram pressure" instability described has been the subject of a linear stability analysis by Ogani and co-workers (A&A 1993), showing that this configuation is indeed unstable.

Williams: How big a wind velocity contrast would you need to produce Kelvin-Helmholtz instabilities?

Stevens: At a velocity contrast of around a factor 2 there is substantial growth of the Kelvin-Helmholtz instability. At a velocity contrast of 1.1 there is little evidence of much growth in the K-H instability. Most WR + O star binaries have only moderate velocity contrasts.

https://doi.org/10.1017/S0074180900202519 Published online by Cambridge University Press